

## Supplementary Information for “First-Principles Study of O<sub>2</sub> Reduction on BaZr<sub>1-x</sub>Co<sub>x</sub>O<sub>3</sub> Cathode in Protonic-Solid Oxide Fuel Cells”

Zhenbin Wang<sup>a</sup>, Wenqiang Yang<sup>a</sup>, Zhuoying Zhu<sup>a</sup>, Ranran Peng<sup>\*a,c</sup>, Xiaojun Wu<sup>\*a,b,c</sup>, Changrong Xia<sup>a</sup> and Yalin Lu<sup>\*a,b,c</sup>

<sup>a</sup> CAS Key Laboratory of Materials for Energy Conversion, Department of Materials Science and Engineering, University of Science and Technology of China, Hefei, 230026, P. R. China.

<sup>b</sup> Hefei National Laboratory of Physical Science at the Microscale, Hefei, 230026, P. R. China.

<sup>c</sup> Synergetic Innovation Center of Quantum Information & Quantum Physics, University of Science and Technology of China, Hefei, 230026, P. R. China.

**Table S1** Summary of calculated surface energies of BZO and BZCO (111), (110), and (100). The two values of BZCO(100) surface energy refer to CoO-terminated surface and ZrO-terminated surface, respectively.

Surface energy (J/m <sup>2</sup> )	100	110	111
BZO	1.02	3.25	2.11
BZCO	0.88/0.95	1.83	1.79

**Table S2** The calculated Bader charges (unit, *e*) of the atoms in several selected configurations. Here, **bulk** and **surface** refer to the bulk and the (100) surface of BZCO; **-p** and **-d** indicate the perfect (-p) and the defect BZCO (-d) system with an oxygen vacancy; **Vac-O<sub>2</sub>** denotes an configuration with an O<sub>2</sub> adsorbed on the BZCO (100) surface (as shown in Fig. 4); and **bulk-H1** presents the bulk of BZCO with a proton defect. The two values in one Co's column are the Bader Charges of the two Co dopants in the considered structures.

Methods	Configurations	Bader charges (e) of atoms					
		Ba	Zr	Co	O	O <sub>2</sub>	H
DFT	bulk-p	1.56	2.21	1.45/1.48	-1.20	-	-
	bulk-d	1.54	2.21	1.18/1.19	-1.22	-	-
	surface-p	1.55	2.20	1.41/1.47	-1.19	-	-
	surface-d	1.55	2.20	1.30/1.29	-1.22	-	-
	Co-top-2	1.55	2.20	1.48/1.38	-1.20	-0.36/-0.39	-
	bulk-H1	1.56	2.21	1.34/1.34	-1.21	-	0.55

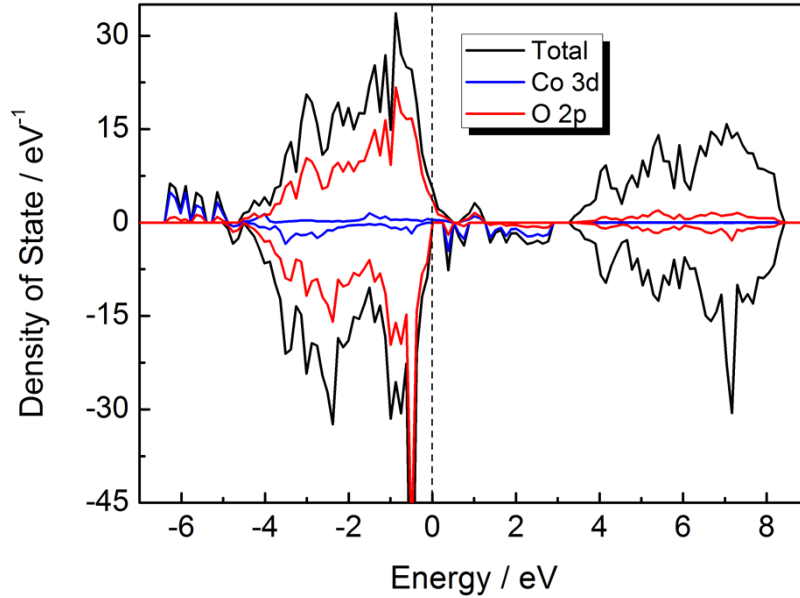


**Fig. S1** Density of State (DOS) of  $\text{BaZr}_{0.75}\text{Co}_{0.25}\text{O}_3$  with PBE + U ( $U = 3.3$  eV).

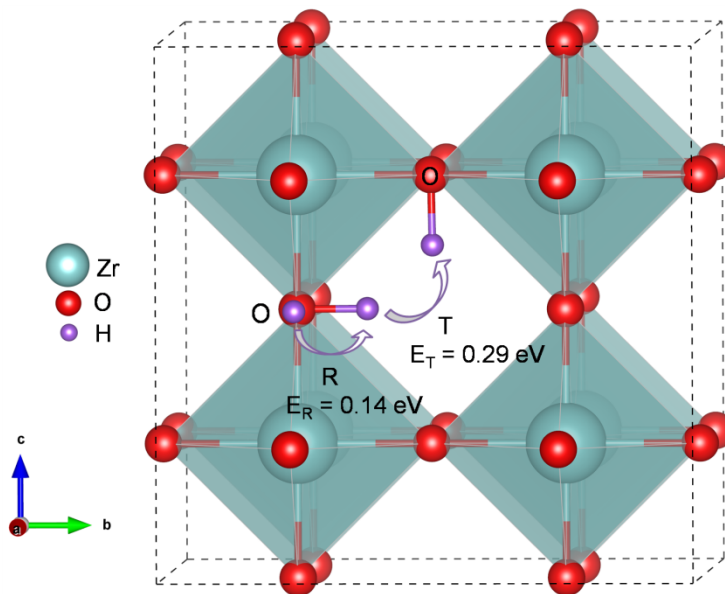


**Fig. S2.** Proton diffusion pathways in  $\text{BaZrO}_3$ , including proton reorientation (R) at an oxygen site of octahedron and transfer (T) between two oxygen sites of intraoctahedron.  $E_R$  and  $E_T$  refer to the hydrogen reorientation barrier around the oxygen of an octahedron and hydrogen transfer between two oxygen of an octahedron.

### S3.2 Oxygen bulk transport properties in the cathode of $\text{BaZr}_{1-x}\text{Co}_x\text{O}_3$ ( $x = 0, 0.25$ ) in dry atmosphere

As depicted in Fig. S3, four sorts of defect sites are differentiated in the supercell of BZCO. The formation energies of these four defects (oxygen vacancies) and the oxygen ion migration barriers between these defects are calculated, shown in Table S2. Whereas, only one kind of defect site exists in BZO in that all oxygen sites are equivalent. The oxygen vacancy formation energy and migration barrier (refer to Table S2) in BZO are 6.39 eV and 1.76 eV, respectively, of which the

migration barrier is much higher than the value ( $0.65 \text{ eV}^1$ ) of atomistic modeling.

The formation energy of oxygen vacancies in BZCO ranges from 1.64 eV to 2.58 eV, which is significantly smaller than that of BZO. Besides, the highest oxygen migration barrier (1.21 eV) of BZCO is also lower than that of BZO. Both case evidence that the Co doping crucially facilitates oxygen transporting in the bulk BZCO cathode. A close examination of oxygen vacancy formation energies of BZCO suggests that the oxygen vacancy between two doping Co species is the easiest one to create, which is the same as that on the BZCO(100) cathode surface.

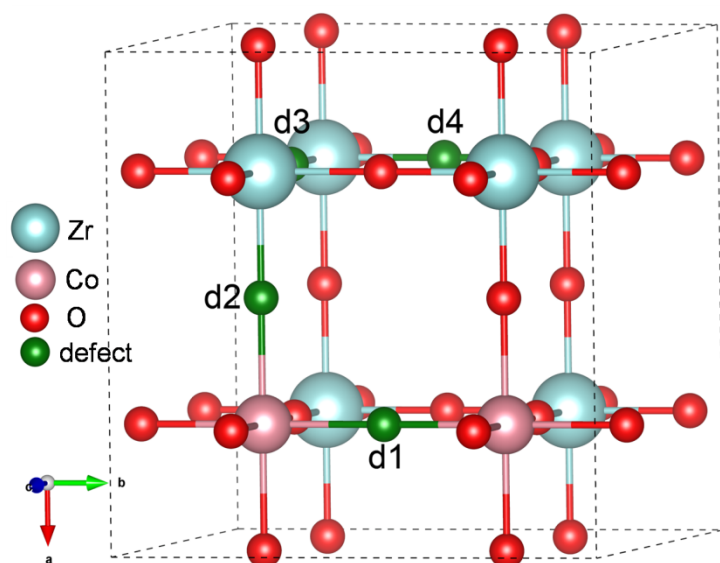


**Fig. S3** Illustration of the possible locations of an oxygen vacancy in BZCO, where  $d_n$  ( $n = 1, 2, 3, 4$ ) denotes a defect site of an oxygen vacancy.

**Table S3** Oxygen vacancy formation energies ( $E_{\text{O-vac}}$ ) and migration barriers ( $E_m$ ) of  $\text{BaZr}_{1-x}\text{Co}_x\text{O}_3$  ( $x = 0, 0.25$ ).

$E_{\text{O-vac}} / \text{eV}$		d1	d2	d3	d4	
$\text{BaZr}_{0.75}\text{Co}_{0.25}\text{O}_3$		0.81	1.64	2.58	2.40	
$\text{BaZrO}_3$		6.39	-	-	-	
$E_m / \text{eV}$		Final defect position				
		d1	d2	d3	d4	
$\text{BaZr}_{0.75}\text{Co}_{0.25}\text{O}_3$	Initial defect position	d1	-	1.02	-	-
		d2	0.19	0.62	1.21	-
		d3	-	1.21	0.77	0.74
		d4	-	-	0.56	-
$\text{BaZrO}_3$		d1	1.76	-	-	-

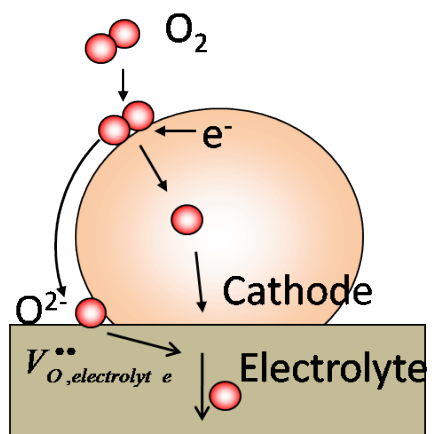


**Fig. S4** Schematic illustration of the  $O_2$  surface reaction and bulk transport on the cathode of  $BaZr_{0.75}Co_{0.25}O_3$ .

### References:

1. S. J. Stokes and M. S. Islam, *Journal of Materials Chemistry*, 2010, **20**, 6258.